# Sb-induced $(1\times1)$ reconstruction on Si(001)

J. R. Power,[1,*] O. Pulci,[2] A. I. Shkrebtii,[1,5] S. Galata,[3] A. Astropekakis,[4] K. Hinrichs,[1,†] N. Esser,[1] R. Del Sole,[2] and W. Richter,[1]

[1] *Institut für Festkörperphysik, Technische Universität Berlin, PN6-1, Hardenbergstrasse 36, D-10623 Berlin, Germany*

[2] *INFM, Department of Physics, University of Rome Tor Vergata, Via della Ricerca Scientifica 1, I-00133 Roma, Italy*

[3] *Department of Physics, Aristotle University of Thessaloniki, Thessaloniki GR-54006, Greece*

[4] *Department of Chemical Engineering, National Technical University of Athens, Athens GR-15780, Greece*

[5] *Department of Physics, University of Toronto, 60 St. Georges Street, Toronto, Ontario, Canada M5S 1A7*

(Received 9 November 2002; published 17 March 2003)

We combine low-energy electron diffraction and reflectance anisotropy spectroscopy (RAS) with *ab initio* calculations of the geometry, band structure, and optical anisotropy to investigate the adsorption of Sb on vicinal Si(001) $(1\times2)$. We focus, in particular, on the controversy concerning the Si(001)-$(1\times1)$-Sb surface. On the basis of total-energy and band-structure calculations, we find that the Sb-undimerised model is unstable and metallic, while experimentally the $(1\times1)$ Sb shows no evidence of a Fermi edge. In contrast, the dimerised $(2\times1)$-Sb and $c(2\times2)$-Sb reconstructions are found to be semiconducting with a minimal difference in total energy. Furthermore, the RAS spectra calculated for both dimerised reconstructions show strong similarities to one another, and agree well with the experimental RAS data for the Sb-induced $(1\times1)$-Sb surface, with a dominant feature centered at 3.7 eV. We report that these findings are compatible with the $(1\times1)$-Sb surface comprising a mixture of the Sb-dimer-terminated $(2\times1)$-Sb and $c(2\times2)$-Sb structures.

DOI: 10.1103/PhysRevB.67.115315 PACS number(s): 73.20.At, 78.40.Fy, 78.66.Db

## I. INTRODUCTION

The interaction of Sb with Si(001) has been widely studied by various techniques owing to its importance in passivating Si surfaces, and especially in behaving as a surfactant for the growth of Ge on Si.[1–8,12,13] Despite this substantial interest, there is still considerable disagreement concerning interpretation of the surface structures prepared experimentally. With the exception of the well-studied $(2\times1)$-Sb reconstruction, the surface structures induced by Sb adsorption on Si(001) remain unclear.

In order to clarify this issue, we combine low-energy electron diffraction (LEED) and reflectance anisotropy spectroscopy (RAS). While the former characterises surface long-range order, RAS probes short-range order thus yielding structural information even where the diffraction experiment may indicate no order is present. In this study vicinal Si(001) samples, cut so as to favor the dominance of the $(1\times2)$ domain over that of the $(2\times1)$ domain, were used. Such samples offer the advantage over flat Si(001) surfaces of removing the ambiguity associated with measured physical quantities representing the average over two equally populated orthogonal $(1\times2)$ and $(2\times1)$ domains. These experimental techniques are combined with *ab initio* calculations of the geometries, of the electronic band structure and of the optical response. We specifically focus on the controversy concerning the structure of the $(1\times1)$-Sb surface. It has been suggested from photoemission experiments that this surface is an ordered structure comprising undimerised Sb atoms residing in bulklike Si lattice sites,[9–11] although previous scanning tunneling microscopy work has reported that this surface is essentially disordered.[2] Despite this controversy, which has lasted more than a decade, no clear picture for the structure of the $(1\times1)$-Sb surface has emerged.

The existence of the $(1\times1)$-Sb surface as a distinct phase was first reported on the basis of LEED, photoemission, and surface differential reflectivity (SDR) measurements.[9,10] The surface structure was formed by the evaporation of 4 ML (monolayers) of Sb at room temperature followed by annealing to 350 °C for 20 min. Particular features in the SDR spectrum and in the photoemission data unique to the $(1\times1)$ structure proved that the surface could not merely be considered disordered, but must be a distinct phase. Following on this, high-resolution core-level photoemission experiments have shown that a very narrow Si $2p$ bulk component is observed for the $(1\times1)$-Sb phase, indicative of an ideal bulk termination.[11] Based on these results, it was concluded that Sb is undimerised and bulk terminates the Si(001) surface in the $(1\times1)$-Sb phase.

In this work, we show by *ab-initio* calculations that such a bulk terminated $(1\times1)$-Sb structure would be thermodynamically unstable and metallic, while experiments do not show any evidence of metallicity, that is, no Fermi edge was observed.[10] We find that the most stable reconstruction, the $(2\times1)$ Sb, is actually very near in total energy to a $c(2\times2)$-Sb phase, and that both these surface reconstructions are semiconducting. Moreover, experimental RAS data for the $(1\times1)$-Sb surface compare well with the calculated anisotropic optical response from both these structures. Since these two surface structures are so near in total energy, we propose that they are likely to coexist on the surface on a size scale smaller than the coherence length of the LEED experiment, thus preventing the appearance of half-order spots in the LEED images.

## II. EXPERIMENT

The RAS experimental arrangement used in this work is similar to that described by Aspnes and co-workers.[14] For a review of the RAS technique and its applications to many

 

different semiconductor surfaces, see Refs. 15,16. The RAS technique derives its surface sensitivity from measurements of the anisotropy in normal incidence reflectance for light polarized along two major orthogonal axes in cubic crystals. The reflectance difference signal $\Delta R$ is normalized to the average reflectance $R$,

$$\frac{\Delta R}{R} = \frac{R_y - R_x}{R}. \tag{1}$$

In the present geometry, the $y$ crystallographic axis is the surface $[\bar{1}10]$ direction [parallel to the silicon dimers of the Si(001)-$(1\times2)$ clean surface], while the $x$ crystallographic axis is [110] (perpendicular to the silicon dimers).

It has been shown[17] that RAS spectra are already produced with their essential features by a few ordered unit cells. RAS is thus able to indicate a much lower degree of ordering than the LEED diffraction experiment, which instead requires, in general, a much larger ordered array of unit cells (one to two orders of magnitude larger than in RAS). This property will be exploited in the present study. Measurement of a Si(001) double-domain reconstructed surface is indeed different for these two techniques: with LEED, the superposition of the diffraction patterns from each domain, differing only by a 90 deg rotation, indicates the possibility of a higher symmetry while with RAS, the signal of each of the two domains differs in sign, causing signal cancellation through superposition.

The experiments were performed in ultrahigh vacuum with a base pressure of $8\times10^{-11}$ mbar. In vacuum, the vicinal Si(001) samples (cut 4° off [001] towards [110]; resistivity$=20\ \Omega$ cm) were degassed for 8 h at 600 °C using direct heating, and subsequently cleaned by flashing to 1000 °C for 30 sec, while making sure the chamber pressure did not exceed $5\times10^{-10}$ mbar. An optical pyrometer and thermocouple mounted close to the sample holder were used to measure the temperature. Once it is clean, each sample revealed a strong single-domain $(1\times2)$ LEED pattern [Fig.1(a)] with split spots indicative of a clean dimerised surface with a regular array of double-atomic height steps. A RAS spectrum of the clean surface is shown in Fig. 2. It is similar to those previously reported by many authors.[18–21] After the RAS measurements on the clean surface, Sb was deposited (from 0.5ML to 6ML) via a tungsten filament evaporator onto the clean surface held at a temperature of 150 °C. The pressure during Sb deposition did not exceed $1\times10^{-9}$ mbar. The evaporator flux rate was calibrated using a quartz crystal oscillator. Following Sb deposition, each sample was then annealed to 360 °C for 5 min causing desorption of all but the last monolayer of Sb.[9] After cooling to room temperature, an Sb-induced $(1\times1)$ LEED pattern was observed [Fig. 1(b)]. A typical RAS spectrum of such a surface is also shown in Fig. 2. This spectrum is dominated by a positive going feature centered at 3.7 eV, whose amplitude displays a direct dependence on the starting (before annealing) coverage of Sb. Some broad structures lower in amplitude are also observed in the 2.0–3.0 eV energy range, their appearance (energetic position, amplitude) depending on the starting Sb coverage.

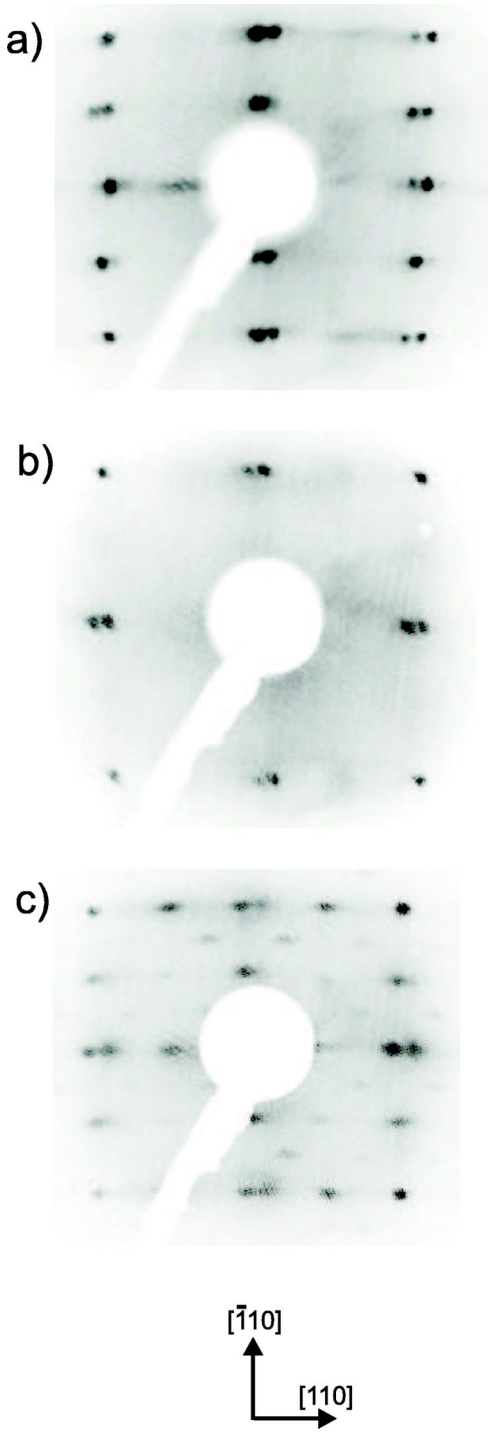


FIG. 1. LEED patterns of (a) clean Si(001) $(1\times2)$ (electron beam energy$=53.4$ eV), (b) $(1\times1)$ Sb (58.1 eV), and (c) $(2\times1)$ Sb surface (58.8 eV) with the presence of some $c(4\times4)$ Sb

Each sample was then further annealed to 610 °C for 5 min and allowed to cool. A double-domain $(2\times1)$ LEED pattern was observed with faint background $c(4\times4)$ spots [Fig. 1(c)]. RAS revealed the removal of the 3.7 eV feature in favor of a small negative going feature at the same energy, along with the disappearance of the structure between 2.0–3.0 eV. Annealing to 1000 °C for 20 sec resulted in the complete desorption of Sb and the reemergence of a clean vicinal

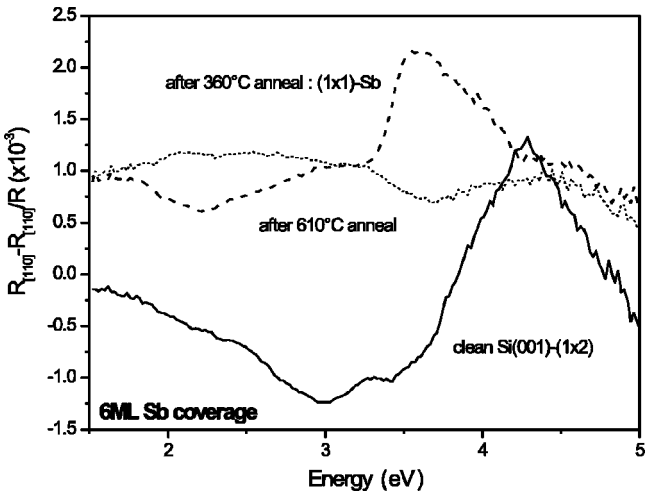


FIG. 2. Experimental RAS spectra for the Sb covered surfaces corresponding to the LEED patterns shown in Fig. 1. For the (1×1)-Sb surface, a spectrum obtained upon a starting deposition of 6 ML is shown.

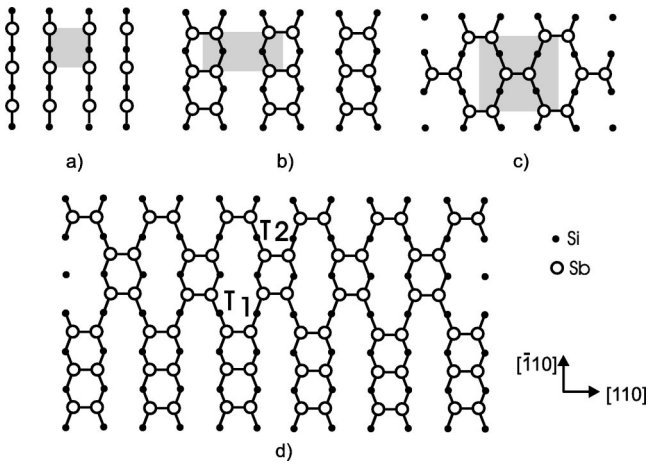


FIG. 3. Structural models of the undimerised (1×1) Sb (a) and the dimer terminated reconstructions, (b) the (2×1) and (c) $c(2\times2)$ reconstructions. Sb atoms are represented by open circles, while the unit cell is indicated by the gray areas. (d) Example for a surface containing both dimerized reconstructions. This would result in the observation of a (1×1) LEED pattern.

Si(001) surface as evidenced by both the characteristic split-spot (1×2) LEED pattern and RAS line shape.

### III. CALCULATIONS

In order to explain the experimental data, we investigated several possible surface geometries using density-functional theory (DFT) within the local density approximation (LDA).[22] The geometries were optimized using a Car-Parrinello plane-waves pseudopotential code.[23] To simulate the surface, slabs consisting of 12 silicon layers were used, terminated at the top and bottom with 1 monolayer of Sb. A plane-wave energy cutoff of 15 Ryd. and a *k*-points mesh equivalent to 32 k points in the (1×1) Brillouin zone (BZ) were employed. The outermost four layers were relaxed, while the inner four layers in the silicon were fixed in their bulk ideal positions. For silicon, the theoretical lattice constant obtained was 5.4 Å, in good agreement with the experimental value of 5.43 Å. The most stable geometries found in our simulations are shown in Fig. 3: they are (b) the (2×1) and (c) $c(2\times2)$ reconstructions. For the purpose of discussion, the (1×1) cell is also shown [see (a) in Fig. 3]. The (2×1) geometry was found to be most stable, although the $c(2\times2)$ was just 0.01 eV per (1×1) surface cell higher in energy. Both these reconstructions were found to be semiconducting [Fig. 4(a), 4(b)]. In contrast, the (1×1) geometry comprising undimerized Sb was revealed to be 0.21 eV per (1×1) surface cell higher in energy than the (2×1) [Fig. 5(a)], and to be metallic [Fig. 5(b)]. The metallic status of this surface can be understood by the fact that Sb has 5 valence electrons: 2 form bonds with Si surface atoms, 2 form a lone pair and one partially occupies a dangling bond. This partially occupied dangling bond gives rise to a partially occupied band and consequently to a metallic surface. However, no evidence of a Fermi edge was found in photoemission experiments for the (1×1) surface.[10] Moreover, it is clear from Fig. 5a that the (1×1) geometry is not even a local minimum of the total energy. If the Sb atoms dimerize, the energy decreases by about 0.4 eV ($=2\times0.21$ eV) per dimer, and the surface becomes semiconducting. Therefore, it appears more likely that the Sb-induced (1×1) surface comprises Sb dimers rather than isolated Sb atoms. The Sb dimers found in the calculation of both the $c(2\times2)$ and (2×1) reconstructions are not buckled and their length is 2.9 Å, approximately twice the Sb covalent radii. The silicon atoms in the underlying layers are almost at their bulk positions due to the long Sb dimer length and longer Si-Sb bonds compared to the clean or As covered Si(001) (2×1). These results are in agreement with previous calculations,[24–26] and could explain why a very narrow $2p$ bulk component was found in core-level shift experiments.[11]

RAS data have been calculated within DFT-LDA for the stable (2×1) and $c(2\times2)$ structures using a *k* points mesh of 64 *k* points in the irreducible part of the Brillouin zone. In order to correct the electronic gap underestimation in DFT, a *GW* calculation was performed.[27,28] For Sb as well as Si states—quite independent of the nature of the states—an

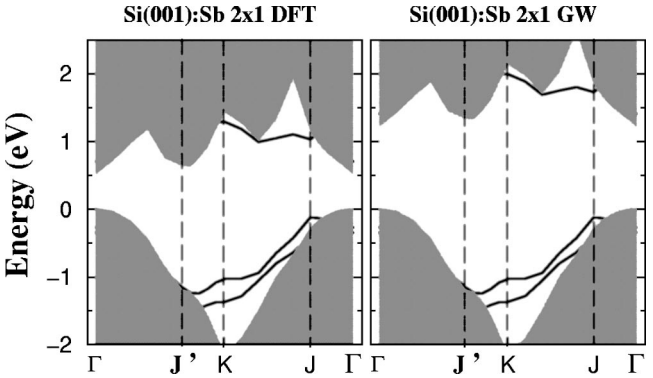


FIG. 4. (a) DFT-LDA band structure for Si(001):Sb(2×1). (b) The same as in (a), but with GW corrections.

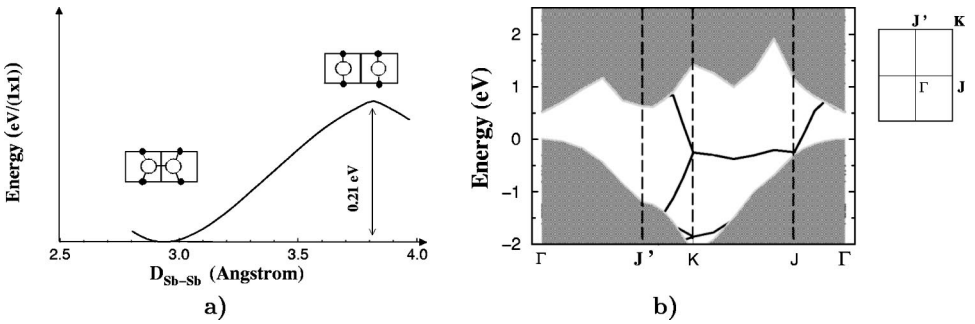


FIG. 5. (a) Total energy as a function of Sb-Sb distance. (b) DFT-LDA band structure for the undimerized $(1\times1)$ structure calculated in a $(2\times1)$ supercell.

opening of the gaps of about 0.6–0.7 eV was found. These *GW* values were consequently used in Figs. 4 and 6.

The calculated RAS spectra are shown in Fig. 6. The $(2\times1)$ and $c(2\times2)$ spectra are quite similar, both showing a dominant peak at approximately 3.9 eV. Through analysis of the calculated data, this peak is found mainly to arise from transitions from Sb-Sb dimer states to Sb and Si backbond states. The negative structure near 2 eV is mainly due to Sb related surface states around the *K* point.

## IV. DISCUSSION

Comparing the experimental data (Fig. 2) with the theoretical results (Fig. 6), the calculated RAS line shapes for the dimer terminated $c(2\times2)$-Sb and $(2\times1)$-Sb surfaces show strong similarities with the experimental RAS line shape for a surface which displays a $(1\times1)$ LEED pattern, particularly in the region of 3.7 eV. Although this result suggests that the $(1\times1)$ surface and the calculated dimer structures are very similar, the question remains how such a Sb dimerized surface fails to produce any half-order LEED periodicity. In order to answer this question, we note that the energy difference between the $(2\times1)$-Sb and the $c(2\times2)$-Sb reconstruction is found to be very small, the $c(2\times2)$ reconstruction, as stated above, being just 0.01 eV higher in energy at 0 K. In the $(2\times1)$ structure, shown in Fig. 3(b), all dimers are equivalent, forming straight dimer chains along $[\bar{1}10]$. We call these as "type 1 (T1)" dimers. In the $c(2\times2)$ structure shown in Fig. 3(c) each second dimer in the chain is shifted along [110]. We call the shifted dimers as "type-2 (T2)" dimers. The almost perfect energetic equivalence of the two structures suggests that any stack of $T1$ and $T2$ dimers is possible. We can have, for instance, $nT1$ dimers, followed (along $[\bar{1}10]$) by $mT2$ dimers, then $n'T1$ dimers and $m'T2$, and so on. The $(2\times1)$ structure has all $n$ equal 1, and all $m$ equal 0. The $c(2\times2)$ structure has all $n$ and $m$ equal 1. A possible stack of $T1$ and $T2$ dimers is sketched in Fig. 3(d). If the $n$'s and $m$'s are large, different $(2\times1)$ domains shifted along [110] with respect to each other will exist, with sizes larger than the coherence length of LEED. In this case each domain will yield the same $(2\times1)$ LEED pattern. If, instead, the $n$'s and $m$'s are randomly distributed and small, so that both $T1$ and $T2$ dimers are present within the LEED coherence length, it follows[29] that the half-order spots will average to zero, and that a $(1\times1)$ LEED pattern will result. Hence, we conclude that in the deposition process, both reconstructions may be created, since the formation of a dimer displaced by one lattice constant in a neighboring row is possible with only a small expense of energy. An example of such surface reconstruction mixing is shown in Fig. 3(d). Such mixing effectively removes any observable LEED half-order periodicity so that only bulk $(1\times1)$ spots remain in the LEED pattern. Hence, a $(1\times1)$ diffraction pattern is compatible with the existence of Sb dimers, which are suggested by the RAS spectra and total-energy calculations. This structure is also compatible with the very narrow Si $2p$ component observed in Ref. 11, since subsurface Si atoms are almost in their ideal positions.

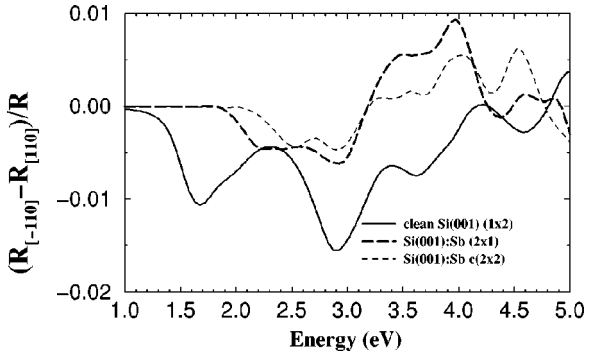


FIG. 6. Calculated RAS spectra for the $c(2\times2)$-Sb, $(2\times1)$-Sb, and the clean $(1\times2)$-Si surfaces.

The fact that the $(2\times1)$ Sb is slightly favored in energy terms over the $c(2\times2)$ Sb explains also why through higher-temperature annealing, the remaining Sb stabilizes in a $(2\times1)$ reconstruction. Similarly, the appearance at higher temperatures of a $c(4\times4)$, which was described in the experiments of Dixon *et al.*[30] with an "overlayer above row dimer" model (Fig. 2(a) of Ref. 30) is plausible on the basis of a dimerized starting surface.

The disappearance of the $(1\times1)$ 3.7 eV structure with higher-temperature annealing (610 °C) can be explained upon consideration of the resulting double-domain $(2\times1)$-Sb LEED pattern observed after this anneal [see Fig. 1(c)]. The observation of a double-domain LEED pattern indicates that the domain ratio must have deteriorated considerably during this anneal. While before Sb deposition, a $(1\times2)$: $(2\times1)$ domain ratio of 3:1 was measured for the clean Si(001)-$(1\times2)$ surface (estimated from intensity measurements of the LEED half-order spot intensities), the domain ratio after this high-temperature anneal appears close to 1:1. Of course in such a situation, the anisotropic signals now strongly compensate. As a consequence, comparison with the

calculated (2×1)-Sb surface is meaningless, since a perfect one-domain structure is assumed there. The appearance of the $c(4\times4)$ and moreover, the direct contribution of steps to the RAS signal, especially for energies below 3 eV, have also to be considered.[18] We note that the RAS spectrum shows no evidence of a step contribution below 3 eV suggesting that Sb could also be decorating the steps. Annealing to 1000 °C desorbs all remaining Sb thus reestablishing the original clean Si(001) domain imbalance as confirmed by measurement of an RAS spectrum characteristic of clean Si(001) (1×2).

## V. CONCLUSION

In conclusion, we have used the complementary information supplied through experimental LEED and RAS data together with *ab-initio* calculations to show that the controversial (1×1)-Sb surface comprises Sb dimers oriented in the [110] direction. The absence of Sb dimer related half-order spots is explained in terms of the random occupation of two energetically similar reconstructions differing only by a lateral shift in Sb dimer position along the [110] direction.

## ACKNOWLEDGMENTS

We thank the DAAD and CRUI for financial support within the Vigoni program. J.R.P acknowledges financial support from the Alexander Von Humboldt foundation. Authors from the TU-Berlin acknowledge the technical assistance of K. Fleischer. O.P. acknowledges Ari P. Seitsonen for useful discussions, and INFM PRA 1-MESS for financial support. Computer facilities at CINECA granted by INFM are gratefully acknowledged.

*Present address: Infineon Technologies, TD-L, Königsbrucker Strasse 105, Dresden D-01069, Germany.

†Present address: Institut für Spektrochemie und angewandte Spektroskopie (ISAS), Albert Einstein Strasse 9, Berlin-Adlershof, D-12489, Germany.

[1] D.H. Rich, T. Miller, G.E. Franklin, and T.-C. Chiang, Phys. Rev. B **39**, 1438 (1989).

[2] D.H. Rich, F.M. Leibsle, A. Samsavar, E.S. Hirschorn, T. Miller, and T.-C. Chiang, Phys. Rev. B **39**, 12 758 (1989).

[3] M. Richter, J.C. Woicik, J. Nogami, P. Pianetta, K.E. Miyano, A.A. Baski, T. Kendelewicz, C.E. Boudlin, W.E. Spicer, C.F. Quate, and I. Lindau, Phys. Rev. Lett. **65**, 3417 (1990).

[4] J. Nogami, A.A. Baski, and C.F. Quate, Appl. Phys. Lett. **58**, 475 (1991).

[5] W.F.J. Slijkerman, P.M. Zagwijn, J.F. van der Veen, D.J. Gratesteijn, and G.F.A. van der Walle, Surf. Sci. **262**, 25 (1992).

[6] M.W. Grant, P.F. Lyman, J.H. Hoogenraad, and L.E. Seiberling, Surf. Sci. **279**, L180 (1992).

[7] M. Copel, M.C. Reuter, E. Kaxiras, and R.M. Tromp, Phys. Rev. Lett. **63**, 632 (1989).

[8] M. Horn-von Hoegen, A. Al Falou, B.H. Muller, U. Kohler, L. Andersohn, B. Dahlheimer, and M. Henzler, Phys. Rev. B **49**, 2637 (1994).

[9] A. Cricenti, S. Selci, A.C. Felici, L. Ferrari, G. Continni, and G. Chiarotti, Phys. Rev. B **47**, 15 745 (1993).

[10] A. Cricenti, H. Bernhoff, D. Purdie, and B. Reihl, J. Vac. Sci. Technol. A **12**, 2327 (1994).

[11] A. Cricenti, P. Perfetti, and G. Le Lay, Surf. Sci. **401**, 427 (1998).

[12] Y.J. Lee, J.W. Kim, and S. Kim, J. Phys.: Condens. Matter **9**, L583 (1997).

[13] B. Garni, I.I. Kravchenko, and C.T. Salling, Surf. Sci. **423**, 43 (1999).

[14] D.E. Aspnes *et al.*, Phys. Rev. Lett. **61**, 2782 (1988).

[15] Edited by G. Bauer and W. Richter, *Optical Characterization of Epitaxial Semiconductor Layers* (Springer-Verlag, Berlin, Heidelberg, 1996).

[16] W. Richter, Appl. Phys. A **75**, 129 (2002).

[17] B. Mendoza *et al.*, Phys. Rev. B. (to be published).

[18] S.G. Jaloviar, J.-L. Lin, F. Liu, V. Zielasek, L. McCaughan, and M.G. Lagally, Phys. Rev. Lett. **82**, 791 (1999).

[19] J.R. Power, P. Weightman, S. Bose, A.I. Shkrebtii, and R. Del Sole, Phys. Rev. Lett. **80**, 3133 (1998).

[20] L. Kipp, D.K. Biegelsen, J.E. Northrup, L.-E. Swartz, and R.D. Bringans, Phys. Rev. Lett. **76**, 2810 (1996).

[21] T. Yasauda, L. Mantese, U. Rossow, and D.E. Aspnes, Phys. Rev. Lett. **74**, 3431 (1995).

[22] W. Kohn and L.J. Sham, Phys. Rev. **140**, A1113 (1965); P. Hohenberg and W. Kohn, Phys. Rev. **136**, B864 (1964); D.M. Ceperley and B.J. Alder, Phys. Rev. Lett. **45**, 566 (1980); J.P. Perdew and A. Zunger, Phys. Rev. B **23**, 5048 (1981).

[23] M. Bockstedte, A. Kley, J. Neugebauer, and M. Scheffler, Comput. Phys. Commun. **107**, 187 (1997).

[24] S.J. Jenkins and G.P. Srivastava, Surf. Sci. **352-354**, 411 (1996); Phys. Rev. B **56**, 9221 (1997).

[25] S. Tang and A.J. Freeman, Phys. Rev. B **47**, 1460 (1993); **48**, 8068 (1993).

[26] J.-H. Cho and M.-H. Kang, Phys. Rev. B **51**, 5058 (1995).

[27] L. Hedin and S. Lundqvist, in *Solid State Physics*, edited by H. Ehrenreich, F. Seitz, and D. Turnbull (Academic, New York, 1969), Vol. 23, p. 1; for a review see F. Aryasetiawan and O. Gunnarsson, Rep. Prog. Phys. **61**, 237 (1998).

[28] GW corrections have been calculated using a slab of 6 silicon layers, terminated on the top with Sb and on the bottom with *H*. We used 797 plane waves, 800 empty bands, and 13-k points in the irreducible BZ. The screen $\epsilon(q)_{G,G'}$ has been calculated within a plasmon pole approximation using 13*q* points in the irreducible BZ. For the exchange part of the self-energy and for $V_{xc}$ we have used 3161 plane waves.

[29] O. Pulci, J. Power, A. Shkrebtii, W. Richter, and R. Del Sole, Comp. Mat. Sci. (to be published).

[30] R.J. Dixon, C.F. McConville, S.J. Jenkins, and G.P. Srivastava, Phys. Rev. B **57**, R12701 (1998).